# TECHNICAL RESEARCH REPORT

S Y S T E M S
R E S E A R C H
C E N T E R

*Supported by the National Science Foundation Engineering Research Center Program (NSFD CD 8803012), Industry and the University*

# Jacobian and Stiffness Analysis of a Novel Six-DOF Parallel Minimanipulator

*by F. Tahmasebi, L-W. Tsai*

TR 92-8

# Jacobian and Stiffness Analysis of a Novel Six-DOF Parallel Minimanipulator

Farhad Tahmasebi* Lung-Wen Tsai†

## Abstract

The Jacobian and stiffness matrices of a novel, six-DOF parallel minimanipulator are derived. The minimanipulator consists of three inextensible limbs, each of which is driven by a five-bar linkage to improve its positional resolution and stiffness. All of the minimanipulator actuators are base-mounted. It is shown that, at the central configuration of the minimanipulator workspace, the stiffness matrix can be diagonalized (decoupled). It is also shown that the minimanipulator can be designed to possess direct or torsional isotropic stiffness properties. Moreover, velocity relationships for the minimanipulator drivers are derived and guidelines for obtaining high stiffness are established.

*Mechanical Engineer, Robotics Branch, NASA/Goddard Space Flight Center, Greenbelt, MD 20771; Associate Member of ASME

†Professor, Mechanical Engineering Dept. and Systems Research Center, University of Maryland, College Park, MD 20742; Member of ASME

# 1 Introduction

Parallel mechanisms have been used for applications in which the requirements for accuracy, rigidity, load-to-weight ratio, and load distribution are more important than the need for a large workspace.

Stewart (1965) introduced his famous six-degree-of-freedom (six-DOF) platform as a motion simulator. Recently, many researchers have suggested the Stewart platform as a robot manipulator (e.g., Hunt, 1983; Fichter, 1986). Other six-DOF parallel manipulators have also been introduced and studied in the literature (e.g., Kohli et al., 1988; Hudgens and Tesar, 1988; Tsai and Tahmasebi, 1991a).

Dualities of serial and parallel manipulators were demonstrated by Waldron and Hunt (1987). For example, inverse kinematics of a serial manipulator is much more difficult than its direct kinematics; whereas, for a parallel manipulator, the opposite is true. Closed-form solutions have been obtained for direct kinematics of certain parallel manipulators (e.g., Griffis and Duffy, 1989; Nanua et al., 1990; Innocenti and Parenti-Castelli, 1990; Tahmasebi and Tsai, 1991).

Gosselin and Angeles (1988, 1989) considered isotropy of the Jacobian matrix in optimum kinematic design of planar and spherical three-DOF parallel manipulators. Arai et al. (1990) also used the Jacobian matrix in optimal design of a six-DOF parallel manipulator. Stiffness matrices of parallel manipulators, which are closely related to their Jacobian matrices, have been studied by Kerr (1989) and Gosselin (1990).

In this paper, the expressions for the Jacobian and stiffness matrices of a three-limbed, six-DOF parallel minimanipulator are derived. The minimanipulator was introduced by Tsai and Tahmasebi (1991a, 1991b) to obtain high positioning resolution and high stiffness in fine-manipulation operations.[1] In addition, the stiffness matrix at the central configuration of

[1]A patent application has been filed for the minimanipulator.

the minimanipulator and velocity relationships for the minimanipulator drivers are used in establishing design guidelines.

## 2 Description of the Minimanipulator

*Let subscript $i$ in this section and the rest of this work represent numbers 1, 2, and 3 in a cyclic manner.* The minimanipulator contains three inextensible limbs, $P_iR_i$, as shown in Figure 1. The lower end of each limb is connected to a simplified five-bar linkage driver and can be moved freely on the base plate. The desired minimanipulator motion is obtained by moving the lower ends of its three limbs on its base plate. Two-DOF universal joints connect the limbs to the moving platform. The lower ends of the limbs are connected to the drivers through three more universal joints. Note that one of the axes of the upper universal joint is collinear with the limb, while the other axis of the upper universal joint as well as one of the axes of the lower universal joint are always perpendicular to the limb. This arrangement is kinematically equivalent to a limb with a spherical joint at its lower end and a revolute joint at its upper end, as shown in Figure 2. The minimanipulator drivers are shown in Figure 3. Point $C_i$ is the output point of a driver. At point $D_i$, there is an actuator on each side of the base plate to drive links $D_iA_i$ and $D_iB_i$. The simplified five-bar drivers are completely symmetric. That is

$$\left|\overline{D_iA_i}\right| = \left|\overline{D_iB_i}\right| = a \tag{1}$$

$$\left|\overline{A_iC_i}\right| = \left|\overline{B_iC_i}\right| = b \tag{2}$$

As a result, coordination between actuator rotations can be easily accomplished. Namely, angular displacement of an output point $C_i$ is obtained by equal actuator rotations, and its radial displacement is obtained by equal and opposite actuator rotations.

Simplified five-bar linkages and inextensible limbs are used to improve positional resolution and stiffness of the minimanipulator. Since the minimanipulator actuators are base-mounted; higher payload capacity, smaller actuator sizes, and lower power dissipation can be obtained. In addition, to achieve even load distribution, the minimanipulator is made completely symmetric. Namely, both triangles $D_1D_2D_3$ and $P_1P_2P_3$ are made equilateral and the joint axes at points $P_1, P_2$, and $P_3$ are made parallel to lines $P_2P_3, P_1P_3$, and $P_1P_2$, respectively.

Instead of simplified five-bar linkages, other two-DOF mechanisms such as regular five-bar linkages, pantographs, bidirectional linear stepper motors, or X-Y positioning tables can be used as drivers for the minimanipulator (Tsai and Tahmasebi, 1991a).

# 3 Jacobian Analysis

First, let us define the fixed base reference frame (XYZ) and the moving platform reference frame (UVW). The base reference frame is shown in Figure 3. The origin of the base reference frame (point O) is placed at the centroid of triangle $D_1D_2D_3$ . The positive X-axis is parallel to and points in the direction of vector $\overline{D_2D_3}$. The positive Y-axis points from point O to point $D_1$. The Z-axis is defined by the right-hand-rule. Similarly, the origin of the platform reference frame (point G) is placed at the centroid of triangle $P_1P_2P_3$ (see Figure 4). The positive U-axis is parallel to and points in the direction of vector $\overline{P_2P_3}$. The positive V-axis points from point O to point $P_1$. The W-axis is defined by the right-hand-rule.

In this paper, without loss of generality, we let $Z_{R,i} = 0$. If $Z_{R,i} > 0$ for a minimanipulator, a simple transformation should be applied to the coordinates of the points used in the following derivations.

Referring to Figure 5, we can write the following vector equation

$$\overline{OR_i} = \overline{OG} + \overline{GP_i} + \overline{P_iR_i} \tag{3}$$

Taking the time derivative of both sides of the above equation with respect to the base reference frame yields

$$^{B}\overline{V}^{R_i} = {}^{B}\overline{V}^{G} + {}^{B}\overline{\omega}^{P} \times \overline{GP_i} + {}^{B}\overline{\omega}^{L_i} \times \overline{P_iR_i} \tag{4}$$

where $\overline{V}$ and $\overline{\omega}$ denote linear and angular velocities, respectively. The right superscript for a velocity vector stands for a point or a rigid body, whereas the left superscript refers to a reference frame in which the velocity is expressed. The base, the platform, and limb $\overline{P_iR_i}$ reference frames (rigid bodies) are denoted by B, P, and $L_i$, respectively. The terms rigid body and reference frame are used interchangeably, because every rigid body can be used as a reference frame and every reference frame can be viewed as a massless rigid body (Kane and Levinson, 1985). Angular velocity of limb $\overline{P_iR_i}$ in the base reference frame can be found from

$$^{B}\overline{\omega}^{L_i} = {}^{P}\overline{\omega}^{L_i} + {}^{B}\overline{\omega}^{P} \tag{5}$$

As shown in Figure 5, let $\eta_i$ be the angle from vector $\overline{GP_i}$ to vector $\overline{P_iR_i}$ measured about a unit vector $\overline{\Gamma}_i$ which is collinear with the axis of the revolute joint at point $P_i$ and points in the direction of vector $\overline{P_{i+2}P_{i+1}}$.[2] Then

$$^{B}\overline{\omega}^{L_i} = \dot{\eta}_i\overline{\Gamma}_i + {}^{B}\overline{\omega}^{P} \tag{6}$$

where $\dot{\eta}_i$ is the time-derivative of $\eta_i$. Substituting the above expression for $^{B}\overline{\omega}^{L_i}$ in equation (4), we obtain

$$^{B}\overline{V}^{R_i} = {}^{B}\overline{V}^{G} + {}^{B}\overline{\omega}^{P} \times \overline{GP_i} + (\dot{\eta}_i\overline{\Gamma}_i + {}^{B}\overline{\omega}^{P}) \times \overline{P_iR_i} \tag{7}$$

or

$$^{B}\overline{V}^{R_i} = {}^{B}\overline{V}^{G} + {}^{B}\overline{\omega}^{P} \times \overline{GR_i} + \dot{\eta}_i\overline{\Gamma}_i \times \overline{P_iR_i} \tag{8}$$

[2]The subscripts are cyclic. If $i = 2$, $i+2$ represents 1. If $i = 3$, $i+1$ and $i+2$ represent 1 and 2, respectively.

The Z-component of ${}^{B}\overline{V}^{R_i}$ is equal to zero. Therefore, we can conclude from the above equation that

$$\dot{\eta}_i = -\frac{{}^{B}\overline{V}^{G} \cdot \bar{n}_z + ({}^{B}\overline{\omega}^{P} \times \overline{GR_i}) \cdot \bar{n}_z}{(\overline{\Gamma}_i \times \overline{P_iR_i}) \cdot \bar{n}_z} \tag{9}$$

where $\bar{n}_z$ is a unit vector in the Z-direction. Let

$$\overline{\mu}_i = \overline{\Gamma}_i \times \overline{P_iR_i} \tag{10}$$

Then

$$\dot{\eta}_i = -\frac{\bar{n}_z \cdot {}^{B}\overline{V}^{G} + (\overline{GR_i} \times \bar{n}_z) \cdot {}^{B}\overline{\omega}^{P}}{\mu_{i,z}} \tag{11}$$

where $\mu_{i,z}$ is the Z-component of the vector $\overline{\mu}_i$. Also, let

$$\mu'_{i,x} = \frac{\mu_{i,x}}{\mu_{i,z}} \quad , \quad \mu'_{i,y} = \frac{\mu_{i,y}}{\mu_{i,z}}$$

where $\mu_{i,x}$ and $\mu_{i,y}$ are the X and Y-components of vector $\overline{\mu}_i$, respectively. Substituting equation (11) into equation (8), and solving for the X-component of the resulting equation, we obtain

$${}^{B}V_x^{R_i} = (\bar{n}_x - \mu'_{i,x}\bar{n}_z) \cdot {}^{B}\overline{V}^{G} + [(\overline{GR_i} \times \bar{n}_x) - \mu'_{i,x}(\overline{GR_i} \times \bar{n}_z)] \cdot {}^{B}\overline{\omega}^{P} \tag{12}$$

where ${}^{B}V_x^{R_i}$ is the X-component of vector ${}^{B}\overline{V}^{R_i}$ and $\bar{n}_x$ is a unit vector in the X-direction. Similarly, we can obtain the following equation

$${}^{B}V_y^{R_i} = (\bar{n}_y - \mu'_{i,y}\bar{n}_z) \cdot {}^{B}\overline{V}^{G} + [(\overline{GR_i} \times \bar{n}_y) - \mu'_{i,y}(\overline{GR_i} \times \bar{n}_z)] \cdot {}^{B}\overline{\omega}^{P} \tag{13}$$

where ${}^{B}V_y^{R_i}$ is the Y-component of vector ${}^{B}\overline{V}^{R_i}$ and $\bar{n}_y$ is a unit vector in the Y-direction.

Let us define the $6 \times 1$ twist vector of the platform ($\dot{\bar{x}}$) as

$$\dot{\bar{x}} = \begin{bmatrix} {}^{B}\overline{V}^{G} \\ \\ {}^{B}\overline{\omega}^{P} \end{bmatrix} \tag{14}$$

If the $6 \times 1$ vector of velocity components at the lower ends of the limbs ($\dot{\bar{q}}$) is given by

$$\dot{\bar{q}} = [{}^{B}\overline{V}_x^{R_1},\ {}^{B}\overline{V}_y^{R_1},\ {}^{B}\overline{V}_x^{R_2},\ {}^{B}\overline{V}_y^{R_2},\ {}^{B}\overline{V}_x^{R_3},\ {}^{B}\overline{V}_y^{R_3}]^T \tag{15}$$

Then, we can define the $6 \times 6$ Jacobian matrix ($\tilde{J}$) by

$$\dot{\bar{q}} = \tilde{J}\dot{\bar{x}} \tag{16}$$

Referring to equations (12) and (13), we can express the Jacobian matrix as

$$\tilde{J} = \begin{bmatrix} (\bar{n}_x - \mu'_{1,x}\bar{n}_z)^T & [(\overline{GR_1} \times \bar{n}_x) - \mu'_{1,x}(\overline{GR_1} \times \bar{n}_z)]^T \\ (\bar{n}_y - \mu'_{1,y}\bar{n}_z)^T & [(\overline{GR_1} \times \bar{n}_y) - \mu'_{1,y}(\overline{GR_1} \times \bar{n}_z)]^T \\ (\bar{n}_x - \mu'_{2,x}\bar{n}_z)^T & [(\overline{GR_2} \times \bar{n}_x) - \mu'_{2,x}(\overline{GR_2} \times \bar{n}_z)]^T \\ (\bar{n}_y - \mu'_{2,y}\bar{n}_z)^T & [(\overline{GR_2} \times \bar{n}_y) - \mu'_{2,y}(\overline{GR_2} \times \bar{n}_z)]^T \\ (\bar{n}_x - \mu'_{3,x}\bar{n}_z)^T & [(\overline{GR_3} \times \bar{n}_x) - \mu'_{3,x}(\overline{GR_3} \times \bar{n}_z)]^T \\ (\bar{n}_y - \mu'_{3,y}\bar{n}_z)^T & [(\overline{GR_3} \times \bar{n}_y) - \mu'_{3,y}(\overline{GR_3} \times \bar{n}_z)]^T \end{bmatrix} \tag{17}$$

where superscript $T$ denotes transpose. Let $\bar{J}_1, \bar{J}_2, \ldots, \bar{J}_6$ be the column vectors of $\tilde{J}$. Expanding equation (17), we get

$$\bar{J}_1 = [1, \ 0, \ 1, \ 0, \ 1, \ 0]^T \tag{18}$$

$$\bar{J}_2 = [0, \ 1, \ 0, \ 1, \ 0, \ 1]^T \tag{19}$$

$$\bar{J}_3 = -\left[\mu'_{1,x}, \ \mu'_{1,y}, \ \mu'_{2,x}, \ \mu'_{2,y}, \ \mu'_{3,x}, \ \mu'_{3,y}\right]^T \tag{20}$$

$$\bar{J}_4 = \begin{bmatrix} -\mu'_{1,\mathrm{x}} \left(\mathrm{Y}_{\mathrm{R},1} - \mathrm{Y}_{\mathrm{G}}\right) \\ \mathrm{Z}_{\mathrm{G}} - \mu'_{1,\mathrm{y}} \left(\mathrm{Y}_{\mathrm{R},1} - \mathrm{Y}_{\mathrm{G}}\right) \\ -\mu'_{2,\mathrm{x}} \left(\mathrm{Y}_{\mathrm{R},2} - \mathrm{Y}_{\mathrm{G}}\right) \\ \mathrm{Z}_{\mathrm{G}} - \mu'_{2,\mathrm{y}} \left(\mathrm{Y}_{\mathrm{R},2} - \mathrm{Y}_{\mathrm{G}}\right) \\ -\mu'_{3,\mathrm{x}} \left(\mathrm{Y}_{\mathrm{R},3} - \mathrm{Y}_{\mathrm{G}}\right) \\ \mathrm{Z}_{\mathrm{G}} - \mu'_{3,\mathrm{y}} \left(\mathrm{Y}_{\mathrm{R},3} - \mathrm{Y}_{\mathrm{G}}\right) \end{bmatrix} \tag{21}$$

$$\bar{J}_5 = \begin{bmatrix} -\mathrm{Z_G} - \mu'_{1,\mathrm{x}} \left(\mathrm{X_G} - \mathrm{X_{R,1}}\right) \\ -\mu'_{1,\mathrm{y}} \left(\mathrm{X_G} - \mathrm{X_{R,1}}\right) \\ -\mathrm{Z_G} - \mu'_{2,\mathrm{x}} \left(\mathrm{X_G} - \mathrm{X_{R,2}}\right) \\ -\mu'_{2,\mathrm{y}} \left(\mathrm{X_G} - \mathrm{X_{R,2}}\right) \\ -\mathrm{Z_G} - \mu'_{3,\mathrm{x}} \left(\mathrm{X_G} - \mathrm{X_{R,3}}\right) \\ -\mu'_{3,\mathrm{y}} \left(\mathrm{X_G} - \mathrm{X_{R,3}}\right) \end{bmatrix} \tag{22}$$

$$\bar{J}_6 = \begin{bmatrix} \mathrm{Y_G} - \mathrm{Y_{R,1}} \\ \mathrm{X_{R,1}} - \mathrm{X_G} \\ \mathrm{Y_G} - \mathrm{Y_{R,2}} \\ \mathrm{X_{R,2}} - \mathrm{X_G} \\ \mathrm{Y_G} - \mathrm{Y_{R,3}} \\ \mathrm{X_{R,3}} - \mathrm{X_G} \end{bmatrix} \tag{23}$$

where $(X_{P,i}, Y_{P,i}, Z_{P,i})$, $(X_{R,i}, Y_{R,i}, Z_{R,i})$, and $(X_G, Y_G, Z_G)$ are the coordinates of points $P_i, R_i$, and $G$, respectively. Note that the Jacobian matrix is a function of the minimanipulator configuration and dimensions.

# 4 Stiffness Analysis

From equation (16), we can conclude that

$$\overline{\delta q} = \tilde{J}\overline{\delta x} \tag{24}$$

where $\overline{\delta q}$ and $\overline{\delta x}$ represent displacements of the lower ends of the limbs and the platform, respectively. Equation (16) and the principle of virtual work can be used to derive the following equation (Asada and Slotine, 1986).

$$\overline{\mathcal{F}} = \tilde{J}^T \overline{f} \tag{25}$$

where

$$\overline{\mathcal{F}} = \begin{bmatrix} \overline{F}_P \\ \overline{M}_P \end{bmatrix} \tag{26}$$

where $\overline{F}_P$ and $\overline{M}_P$ are the force and moment applied to the platform and

$$\overline{f} = [f_{1,x},\ \ f_{1,y},\ \ f_{2,x},\ \ f_{2,y},\ \ f_{3,x},\ \ f_{3,y}]^T \tag{27}$$

where $f_{i,x}$ and $f_{i,y}$ are the X and Y-components of the force applied at point $R_i$. The forces and displacements at the lower ends of the limbs are related by the following equation.

$$\overline{f} = \tilde{\kappa}\overline{\delta q} \tag{28}$$

where $\tilde{\kappa}$ is a $6 \times 6$ diagonal matrix whose elements have units of force per unit length. From equations (24), (25), and (28), we can conclude that

$$\overline{\mathcal{F}} = \tilde{J}^T \tilde{\kappa} \tilde{J} \overline{\delta x} \tag{29}$$

In what follows, we set $\tilde{\kappa}$ equal to the $6 \times 6$ identity matrix, because we are only interested in the effect of the minimanipulator dimensions on its stiffness. Therefore, the stiffness matrix for the platform ($\tilde{K}$) is expressed as

$$\tilde{K} = \tilde{J}^T \tilde{J} \tag{30}$$

Note that $\tilde{K}$ is a symmetric, positive semidefinite matrix. Elements of the lower triangular portion of $\tilde{K}$ are given in Appendix A.

## 4.1 Central Stiffness Matrix

In this section, the stiffness matrix at the central configuration of the minimanipulator workspace (central stiffness matrix) will be derived. The central configuration is defined as the configuration where

1. The platform is not rotated with respect to the base.

2. The centroid of triangle $P_1P_2P_3$ (platform) is directly on top of the centroid of triangle $D_1D_2D_3$, i.e. $X_G = Y_G = 0$.

Let $\left|\overline{GP_i}\right| = p$. Also, at the central configuration , let $\left|\overline{OR_i}\right| = \nu$ and $Z_G = \zeta$. Using equations (17) and (30), the stiffness matrix at the central configuration ($\tilde{K}^+$) is found to be

$$\tilde{K}^+ = \begin{bmatrix} 3 & 0 & 0 & 0 & -\frac{3(\nu-2p)\zeta}{2(\nu-p)} & 0 \\ 0 & 3 & 0 & \frac{3(\nu-2p)\zeta}{2(\nu-p)} & 0 & 0 \\ 0 & 0 & \frac{3\zeta^2}{(\nu-p)^2} & 0 & 0 & 0 \\ 0 & \frac{3(\nu-2p)\zeta}{2(\nu-p)} & 0 & \frac{3(\nu^2-2p\nu+2p^2)\zeta^2}{2(\nu-p)^2} & 0 & 0 \\ -\frac{3(\nu-2p)\zeta}{2(\nu-p)} & 0 & 0 & 0 & \frac{3(\nu^2-2p\nu+2p^2)\zeta^2}{2(\nu-p)^2} & 0 \\ 0 & 0 & 0 & 0 & 0 & 3\nu^2 \end{bmatrix} \tag{31}$$

It is desirable to eliminate the off-diagonal terms which couple the forces (moments) applied along (about) the X and Y axes to the rotations (translations) about (along) the Y and X axes, respectively. Fortunately, this can be easily accomplished by setting

$$p = \frac{\nu}{2} \tag{32}$$

In other words, the platform (triangle $P_1P_2P_3$) should be one-half of triangle $R_1R_2R_3$ at the central configuration. The above result is similar to that obtained by Kerr (1989) in designing a Stewart-platform-based force and torque transducer. If the condition expressed in the above equation is satisfied, then

$$\zeta^2 = r^2 - p^2 \tag{33}$$

where $r$ is the length of any limb. If equations (32) and (33) are used to substitute for $\nu$ and $\zeta$ in equation (31), matrix $\tilde{K}^{+}$ reduces to

$$\tilde{K}^{*} = \begin{bmatrix} 3 & & & & & \mathbf{0} \\ & 3 & & & & \\ & & \frac{3(r^2-p^2)}{p^2} & & & \\ & & & 3(r^2-p^2) & & \\ & & & & 3(r^2-p^2) & \\ & \mathbf{0} & & & & 12p^2 \end{bmatrix} \qquad (34)$$

The above equation can be used to determine the relative dimensions of the minimanipulator so that desirable characteristics can be obtained. Note that dimension $\nu$ (the independent variable) can be determined from other requirements and constraints such as maximizing the workspace and the upper bound on size of the base plate.

The diagonal elements of $\tilde{K}^{*}$ ($K^{*}_{1,1}, K^{*}_{2,2}, \ldots, K^{*}_{6,6}$) give indications of how well the input forces or torques are transmitted into forces and torques at the platform (end-effector). The higher these terms, the higher the force-transmission capability (mechanical advantage) of the minimanipulator, and the higher the positional resolution of the minimanipulator. For some applications, it may be desirable to maximize one or more of these stiffness terms. For other applications, the designer may be interested in isotropic stiffness properties. Note that it is not possible to make all of the diagonal stiffness terms equal. However, it will be shown that it is possible to obtain isotropic direct stiffness or isotropic torsional stiffness.

To move the platform in the X or Y-direction, the lower ends of all three limbs should also move in the X or Y-direction. As a result, elements $K^{*}_{1,1}$ and $K^{*}_{2,2}$ are constants. Only the simplified five-bar linkage drivers contribute to increasing the direct stiffness values in the X and Y-directions. Stiffness terms $K^{*}_{3,3}$, $K^{*}_{4,4}$, and $K^{*}_{5,5}$ are functions of two design variables ($r$ and $p$). However, $K^{*}_{6,6}$ is only dependent on variable $p$ (circumradius of the platform). This is related to the fact that in order to rotate the platform about the Z-axis, the lower ends of the limbs should move on a circle, which passes through them, in the same direction and by an equal amount.

The first three diagonal terms of the $\tilde{K}^*$ matrix are direct stiffness terms. Equation (34) shows that by setting

$$r = \sqrt{2}p$$

we can obtain equal direct stiffness values in the $X, Y$, and $Z$ directions. At this configuration, the angle between any of the limbs and the base plane becomes equal to 45 degrees.

The last three diagonal terms of the $\tilde{K}^*$ matrix are torsional stiffness terms. Referring to equation (34), we notice that by setting

$$r = \sqrt{5}p$$

we can obtain equal torsional stiffness values in the $X, Y$, and $Z$ directions. At this configuration, the angle between any of the limbs and the base plane becomes equal to 63.43 degrees.

# 5 Velocity Analysis of the Drivers

Figure 6 shows a simplified five-bar driver. Let $\theta_i$ and $\phi_i$ (driver input angles) be the angles from the positive X-axis to the vectors $\overline{D_iB_i}$ and $\overline{D_iA_i}$, respectively, measured about the positive Z-axis. $D_iB_i$ and $D_iA_i$ are the input links of the driver and vector $\overline{D_iX_{i,1}}$ is parallel to the positive X-axis. In the following analysis, we assume that $\phi_i \geq \theta_i$ (if $\phi_i < \theta_i$, 360 degrees is added to $\phi_i$). In addition, only one branch of a driver is considered, because the other branch can be realized only by disassembling and reassembling the driver. From the driver geometry, we can write

$$\left|\overline{D_iC_i}\right| = a\cos\xi_i + b\cos\vartheta_i \tag{35}$$

where $\xi_i$ is the angle of line $D_iC_i$ with line $D_iB_i$ or line $D_iA_i$ and $\vartheta_i$ is the angle of line $C_iD_i$ with line $C_iB_i$ or line $C_iA_i$. Applying the law of sines to triangle $D_iA_iC_i$, we get

$$\frac{\sin\vartheta_i}{a} = \frac{\sin\xi_i}{b} \tag{36}$$

or

$$\cos\vartheta_i = \sqrt{1-(a/b)^2\sin^2\xi_i} \tag{37}$$

From equations (35) and (37), we conclude that

$$\overline{D_iC_i} = \left[a\cos\xi_i + b\sqrt{1-(a/b)^2\sin^2\xi_i}\right]\bar{n}_{r,i} \tag{38}$$

where $\bar{n}_{r,i}$ is a unit vector in the direction of vector $\overline{D_iC_i}$.

Let $\psi_i$ be the angle from the positive X-axis to the vector $\overline{D_iC_i}$, measured about the positive Z-axis. Also, as shown in Figure 6, let the unit vector $\bar{n}_{t,i}$ be at 90 degrees to the unit vector $\bar{n}_{r,i}$, measured about the positive Z-axis. Taking the time-derivatives of both sides of equation (38), with respect to the base reference frame, we obtain

$$\begin{bmatrix} {}^BV_r^{C_i} \\ {}^BV_t^{C_i} \end{bmatrix} = \tilde{J}_d \begin{bmatrix} \dot{\xi}_i \\ \dot{\psi}_i \end{bmatrix} \tag{39}$$

where

$$\tilde{J}_d = b\begin{bmatrix} -(a/b)\sin\xi_i - (a/b)^2\frac{\sin\xi_i\cos\xi_i}{\sqrt{1-(a/b)^2\sin^2\xi_i}} & 0 \\ 0 & (a/b)\cos\xi_i + \sqrt{1-(a/b)^2\sin^2\xi_i} \end{bmatrix} \tag{40}$$

and $({}^BV_r^{C_i}, {}^BV_t^{C_i})$ are the radial (in the $\bar{n}_{r,i}$ direction) and tangential (in the $\bar{n}_{t,i}$ direction) components of the velocity of point $C_i$. In addition, $\dot{\xi}_i$ and $\dot{\psi}_i$ denote time-derivatives of angles $\xi_i$ and $\psi_i$, respectively. Note that $\dot{\xi}_i$ and $\dot{\psi}_i$ are related to the input speeds ($\dot{\theta}_i$ and $\dot{\phi}_i$) by the following linear relationships.

$$\dot{\theta}_i = \dot{\psi}_i - \dot{\xi}_i \tag{41}$$

$$\dot{\phi}_i = \dot{\psi}_i + \dot{\xi}_i \tag{42}$$

Equations (39) - (42) show that for a given $b$, the smaller the ratio $a/b$, the higher the speed reduction (mechanical advantage) of the driver. Speed reductions by the drivers result in high stiffness for the minimanipulator.

# 6 Design Guidelines

Based on the results of the last two sections, the following design guidelines can be established.

- The central stiffness matrix can be diagonalized (decoupled) by making the platform (triangle $P_1P_2P_3$) one-half of the triangle passing through the lower ends of the limbs, i.e. $p = \nu/2$.
- If the central stiffness matrix is decoupled, then
  - Direct stiffness isotropy can be obtained by making the limb length equal to $\sqrt{2}$ times the circumradius of the platform, i.e. $r = \sqrt{2}p$.
  - Torsional stiffness isotropy can be obtained by making the limb length equal to $\sqrt{5}$ times the circumradius of the platform, i.e. $r = \sqrt{5}p$.
  - The larger the ratio of the limb length to the platform circumradius $(r/p)$, the larger the direct stiffness in the Z-direction.
  - For a given platform size, the larger the limb length, the larger the torsional stiffness values in the X and Y-directions.
  - For a given limb length, the larger the platform size, the smaller the torsional stiffness values in the X and Y-directions, and the larger the torsional stiffness in the Z-direction.

- The smaller the ratio of the input link length to the output link length of a driver $(a/b)$, the higher the stiffness of the minimanipulator.

Note that the minimanipulator will be at or near the center of its workspace during most of its operations. Therefore, establishing design guidelines based on the central stiffness matrix is justified.

# 7 Summary

In this paper, the Jacobian and stiffness matrices of a three-limbed, six-DOF parallel minimanipulator are obtained. The velocity relationships for the minimanipulator drivers are also derived. It is shown that the stiffness matrix at the central configuration of the minimanipulator workspace can be decoupled, if the platform size is made half of the size of the triangle passing through the lower ends of the limbs. It is also shown that, at the central configuration of the minimanipulator, ratio of the limb length to the platform circumradius must be equal to $\sqrt{2}$ ($\sqrt{5}$) for obtaining direct (torsional) stiffness isotropy. Finally, guidelines for obtaining large stiffness values are established.

# Acknowledgments

This research was supported in part by the NSF Engineering Research Center program, NSFD CDR 8803012. The first author gratefully acknowledges the support of NASA/Goddard Space Flight Center. Such supports do not constitute endorsements of the views expressed in the paper by the supporting agencies.

# References


- Arai, T., Cleary, K., Nakamura, T., Adachi, H., and Homma, K., 1990, "Design, Analysis and Construction of a Prototype Parallel Link Manipulator," *Proc. of the IEEE International Workshop on Intelligent Robots and Systems (IROS '90)*, pp. 205-212.

- Asada, H., and Slotine, J.-J.E., 1986, *Robot Analysis and Control*, John Wiley and Sons, New York.

- Fichter, E.F., 1986, "A Stewart Platform-based Manipulator: General Theory and Practical Construction," *Int. J. of Robotics Research*, Vol. 5, pp. 157-182.

- Gosselin, C., and Angeles, J., 1988, "The Optimum Kinematic Design of a Planar Three-Degree-of-Freedom Parallel Manipulator," *Trans. ASME, J. of Mech., Transmis., and Auto. in Design*, Vol. 110, pp. 35-41.

- Gosselin, C., and Angeles, J., 1989, "The Optimum Kinematic Design of a Spherical Three-Degree-of-Freedom Parallel Manipulator," *Trans. ASME. J. of Mech., Transmis., and Auto. in Design*, Vol. 111, pp. 202-207.

- Gosselin, C., 1990, "Stiffness Mapping of Parallel Manipulators," *IEEE Transactions on Robotics and Automation*, Vol. 6, pp. 377-382.

- Griffis, M., and Duffy, J., 1989, "A Forward Displacement Analysis of a Class of Stewart Platforms," *J. of Robotic Systems*, Vol. 6, pp. 703-720.

- Hudgens, J.C., and Tesar, D., 1988, "A Fully-Parallel Six Degree-of-Freedom Micromanipulator: Kinematic Analysis and Dynamic Model," *Trends and Developments in Mechanisms, Machines, and Robotics - Proc. of the 20th Biennial Mechanisms Conference*, ASME, New York, DE-Vol. 15-3, pp. 29-37.

- Hunt, K.H., 1983, "Structural Kinematics of In-Parallel-Actuated Robot-Arms," *Trans. ASME, J. of Mech., Transmis., and Auto. in Design*, Vol. 105, pp. 705-712.
- Innocenti, C., and Parenti-Castelli, V., 1990, "Direct Position Analysis of the Stewart Platform Mechanism," *Mechanism and Machine Theory*, Vol. 25, pp. 611-612.
- Kane, T.R., and Levinson, D.A., 1985, *Dynamics: Theory and Applications*, McGraw-Hill, New York.
- Kerr, D.R., 1989, "Analysis, Properties, and Design of a Stewart-Platform Transducer," *Trans. ASME, J. of Mech., Transmis., and Auto. in Design*, Vol. 111, pp. 25-28.
- Kohli, D., Lee, S.H., Tsai, K.Y., and Sandor, G.N., 1988, "Manipulator Configurations Based on Rotary-Linear (R-L) Actuators and Their Direct and Inverse Kinematics," *Trans. ASME, J. of Mech., Transmis., and Auto. in Design*, Vol. 110, pp. 397-404.
- Nanua, P., Waldron, K.J., and Murthy, V., 1990, "Direct Kinematic Solution of a Stewart Platform," *IEEE Transactions on Robotics and Automation*, Vol. 6, pp. 438-444.
- Stewart, D., 1965, "A Platform with Six Degrees of Freedom," *Proc. Institute of Mechanical Engr.*, London, England, Vol. 180, pp. 371-386.
- Tahmasebi, F., and Tsai, L.W., 1991, "Closed-Form Direct Kinematics Solution of a New Parallel Minimanipulator," *Technical Research Report TR 91-92*, Systems Research Center, University of Maryland, College Park.
- Tsai, L.W., and Tahmasebi, F., 1991a, "Synthesis and Analysis of a New Class of Six-Degree-of-Freedom Parallel Minimanipulators," *Technical Research Report TR 91-83*, Systems Research Center, University of Maryland, College Park.

- Tsai, L.W., and Tahmasebi, F., 1991b, "Design and Analysis of a New Six-Degree-of-Freedom Parallel Minimanipulator," *Proc. of the 6th International Conference on CAD/CAM, Robotics, and Factories of the Future* , Springer-Verlag, Berlin.

- Waldron, K.J., and Hunt, K.H., 1987, "Series-Parallel Dualities in Actively Coordinated Mechanisms," *Proc. of the 4th Int. Symp. on Robotic Research*, MIT press, Cambridge, MA, pp. 175-181.

# Appendix A - Lower Triangular Elements of $\tilde{K}$

$$K_{1,1} = 3$$

$$K_{2,1} = 0$$

$$K_{2,2} = 3$$

$$K_{3,1} = -\mu'_{3,x} - \mu'_{2,x} - \mu'_{1,x}$$

$$K_{3,2} = -\mu'_{3,y} - \mu'_{2,y} - \mu'_{1,y}$$

$$K_{3,3} = {\mu'_{3,y}}^2 + {\mu'_{3,x}}^2 + {\mu'_{2,y}}^2 + {\mu'_{2,x}}^2 + {\mu'_{1,y}}^2 + {\mu'_{1,x}}^2$$

$$K_{4,1} = -\mu'_{3,x}\,(\mathrm{Y_{R,3}} - \mathrm{Y_G}) - \mu'_{2,x}\,(\mathrm{Y_{R,2}} - \mathrm{Y_G}) - \mu'_{1,x}\,(\mathrm{Y_{R,1}} - \mathrm{Y_G})$$

$$K_{4,2} = 3\,\mathrm{Z_G} - \mu'_{3,y}\,(\mathrm{Y_{R,3}} - \mathrm{Y_G}) - \mu'_{2,y}\,(\mathrm{Y_{R,2}} - \mathrm{Y_G}) - \mu'_{1,y}\,(\mathrm{Y_{R,1}} - \mathrm{Y_G})$$

$$\begin{aligned} K_{4,3} = {} & -\mu'_{3,y}\,\left(\mathrm{Z_G} - \mu'_{3,y}\,(\mathrm{Y_{R,3}} - \mathrm{Y_G})\right) - \mu'_{2,y}\,\left(\mathrm{Z_G} - \mu'_{2,y}\,(\mathrm{Y_{R,2}} - \mathrm{Y_G})\right) \\ & -\mu'_{1,y}\,\left(\mathrm{Z_G} - \mu'_{1,y}\,(\mathrm{Y_{R,1}} - \mathrm{Y_G})\right) + {\mu'_{3,x}}^2\,(\mathrm{Y_{R,3}} - \mathrm{Y_G}) \\ & +{\mu'_{2,x}}^2\,(\mathrm{Y_{R,2}} - \mathrm{Y_G}) + {\mu'_{1,x}}^2\,(\mathrm{Y_{R,1}} - \mathrm{Y_G}) \end{aligned}$$

$$\begin{aligned} K_{4,4} = {} & \left(\mathrm{Z_G} - \mu'_{3,y}\,(\mathrm{Y_{R,3}} - \mathrm{Y_G})\right)^2 + \left(\mathrm{Z_G} - \mu'_{2,y}\,(\mathrm{Y_{R,2}} - \mathrm{Y_G})\right)^2 + \\ & \left(\mathrm{Z_G} - \mu'_{1,y}\,(\mathrm{Y_{R,1}} - \mathrm{Y_G})\right)^2 + {\mu'_{3,x}}^2\,(\mathrm{Y_{R,3}} - \mathrm{Y_G})^2 + \\ & {\mu'_{2,x}}^2\,(\mathrm{Y_{R,2}} - \mathrm{Y_G})^2 + {\mu'_{1,x}}^2\,(\mathrm{Y_{R,1}} - \mathrm{Y_G})^2 \end{aligned}$$

$$K_{5,1} = -3\,\mathrm{Z_G} - \mu'_{3,x}\,(\mathrm{X_G} - \mathrm{X_{R,3}}) - \mu'_{2,x}\,(\mathrm{X_G} - \mathrm{X_{R,2}}) - \mu'_{1,x}\,(\mathrm{X_G} - \mathrm{X_{R,1}})$$

$$K_{5,2} = -\mu'_{3,y}\,(\mathrm{X_G} - \mathrm{X_{R,3}}) - \mu'_{2,y}\,(\mathrm{X_G} - \mathrm{X_{R,2}}) - \mu'_{1,y}\,(\mathrm{X_G} - \mathrm{X_{R,1}})$$

$$\begin{aligned}K_{5,3} &= -\mu'_{3,x}\left(-Z_G-\mu'_{3,x}\left(X_G-X_{R,3}\right)\right)-\mu'_{2,x}\left(-Z_G-\mu'_{2,x}\left(X_G-X_{R,2}\right)\right)-\\&\quad \mu'_{1,x}\left(-Z_G-\mu'_{1,x}\left(X_G-X_{R,1}\right)\right)+{\mu'_{3,y}}^2\left(X_G-X_{R,3}\right)+\\&\quad {\mu'_{2,y}}^2\left(X_G-X_{R,2}\right)+{\mu'_{1,y}}^2\left(X_G-X_{R,1}\right)\end{aligned}$$

$$\begin{aligned}K_{5,4} &= -\mu'_{3,y}\left(X_G-X_{R,3}\right)\left(Z_G-\mu'_{3,y}\left(Y_{R,3}-Y_G\right)\right)-\mu'_{2,y}\left(X_G-X_{R,2}\right)\left(Z_G-\mu'_{2,y}\left(Y_{R,2}-Y_G\right)\right)-\\&\quad \mu'_{1,y}\left(X_G-X_{R,1}\right)\left(Z_G-\mu'_{1,y}\left(Y_{R,1}-Y_G\right)\right)-\mu'_{3,x}\left(Y_{R,3}-Y_G\right)\left(-Z_G-\mu'_{3,x}\left(X_G-X_{R,3}\right)\right)-\\&\quad \mu'_{2,x}\left(Y_{R,2}-Y_G\right)\left(-Z_G-\mu'_{2,x}\left(X_G-X_{R,2}\right)\right)-\mu'_{1,x}\left(Y_{R,1}-Y_G\right)\left(-Z_G-\mu'_{1,x}\left(X_G-X_{R,1}\right)\right)\end{aligned}$$

$$\begin{aligned}K_{5,5} &= \left(-Z_G-\mu'_{3,x}\left(X_G-X_{R,3}\right)\right)^2+\left(-Z_G-\mu'_{2,x}\left(X_G-X_{R,2}\right)\right)^2+\\&\quad \left(-Z_G-\mu'_{1,x}\left(X_G-X_{R,1}\right)\right)^2+{\mu'_{3,y}}^2\left(X_G-X_{R,3}\right)^2+\\&\quad {\mu'_{2,y}}^2\left(X_G-X_{R,2}\right)^2+{\mu'_{1,y}}^2\left(X_G-X_{R,1}\right)^2\end{aligned}$$

$$K_{6,1} = -Y_{R,3}-Y_{R,2}-Y_{R,1}+3\,Y_G$$

$$K_{6,2} = X_{R,3}+X_{R,2}+X_{R,1}-3\,X_G$$

$$\begin{aligned}K_{6,3} &= -\mu'_{3,x}\left(Y_G-Y_{R,3}\right)-\mu'_{2,x}\left(Y_G-Y_{R,2}\right)-\mu'_{1,x}\left(Y_G-Y_{R,1}\right)-\\&\quad \mu'_{3,y}\left(X_{R,3}-X_G\right)-\mu'_{2,y}\left(X_{R,2}-X_G\right)-\mu'_{1,y}\left(X_{R,1}-X_G\right)\end{aligned}$$

$$\begin{aligned}K_{6,4} &= \left(X_{R,3}-X_G\right)\left(Z_G-\mu'_{3,y}\left(Y_{R,3}-Y_G\right)\right)+\left(X_{R,2}-X_G\right)\left(Z_G-\mu'_{2,y}\left(Y_{R,2}-Y_G\right)\right)+\\&\quad \left(X_{R,1}-X_G\right)\left(Z_G-\mu'_{1,y}\left(Y_{R,1}-Y_G\right)\right)-\mu'_{3,x}\left(Y_G-Y_{R,3}\right)\left(Y_{R,3}-Y_G\right)-\\&\quad \mu'_{2,x}\left(Y_G-Y_{R,2}\right)\left(Y_{R,2}-Y_G\right)-\mu'_{1,x}\left(Y_G-Y_{R,1}\right)\left(Y_{R,1}-Y_G\right)\end{aligned}$$

$$\begin{aligned}K_{6,5} &= \left(Y_G-Y_{R,3}\right)\left(-Z_G-\mu'_{3,x}\left(X_G-X_{R,3}\right)\right)+\left(Y_G-Y_{R,2}\right)\left(-Z_G-\mu'_{2,x}\left(X_G-X_{R,2}\right)\right)+\\&\quad \left(Y_G-Y_{R,1}\right)\left(-Z_G-\mu'_{1,x}\left(X_G-X_{R,1}\right)\right)-\mu'_{3,y}\left(X_G-X_{R,3}\right)\left(X_{R,3}-X_G\right)-\\&\quad \mu'_{2,y}\left(X_G-X_{R,2}\right)\left(X_{R,2}-X_G\right)-\mu'_{1,y}\left(X_G-X_{R,1}\right)\left(X_{R,1}-X_G\right)\end{aligned}$$

$$K_{6,6} = \left(Y_G-Y_{R,3}\right)^2+\left(Y_G-Y_{R,2}\right)^2+\left(Y_G-Y_{R,1}\right)^2+\left(X_{R,3}-X_G\right)^2+\left(X_{R,2}-X_G\right)^2+\left(X_{R,1}-X_G\right)^2$$

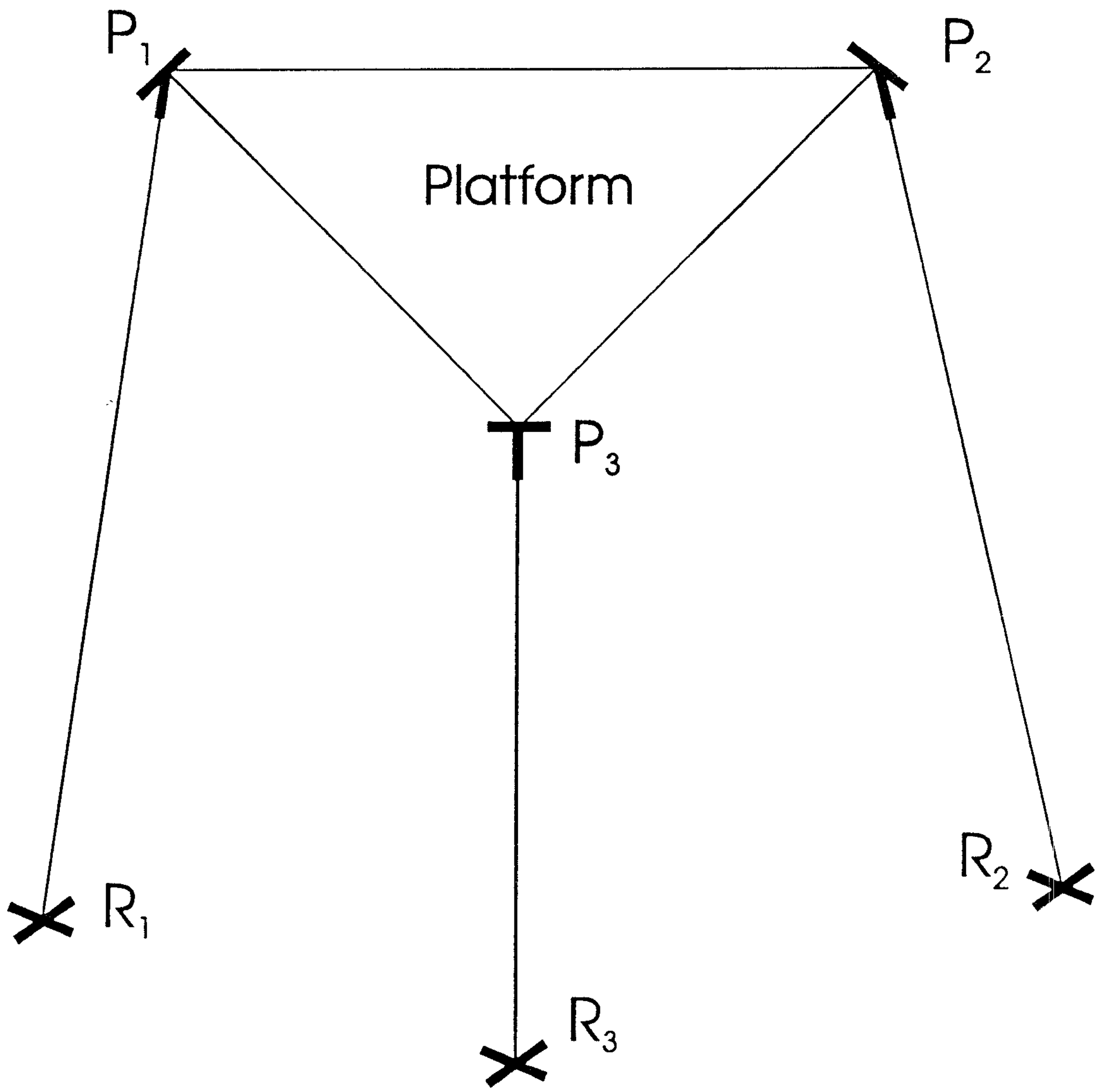


$R_1$, $R_2$, and $R_3$ are connected to drivers.

Figure 1 - Represntation of a Minimanipulator

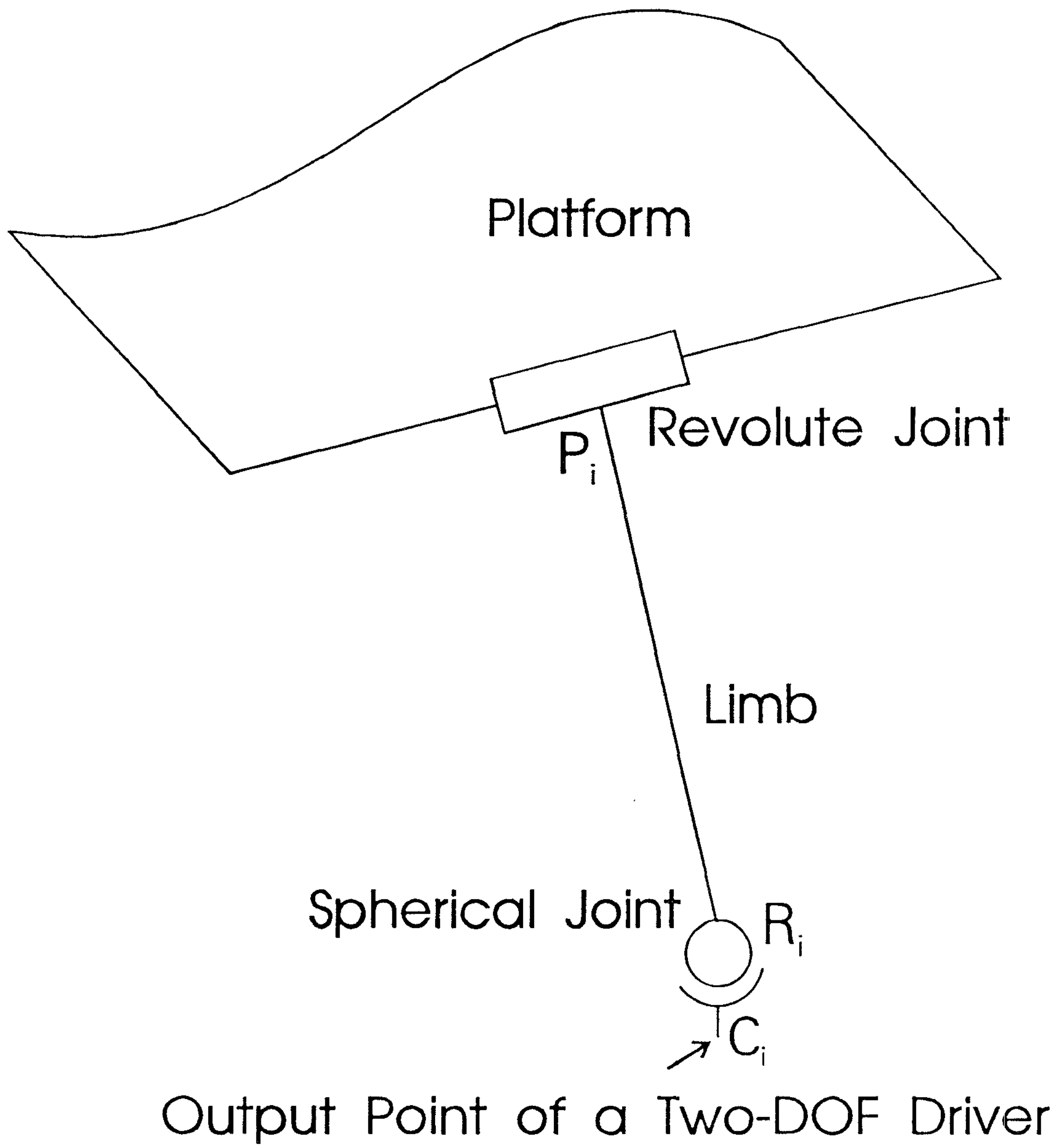


Figure 2 - Kinematic Equivalent of a Limb

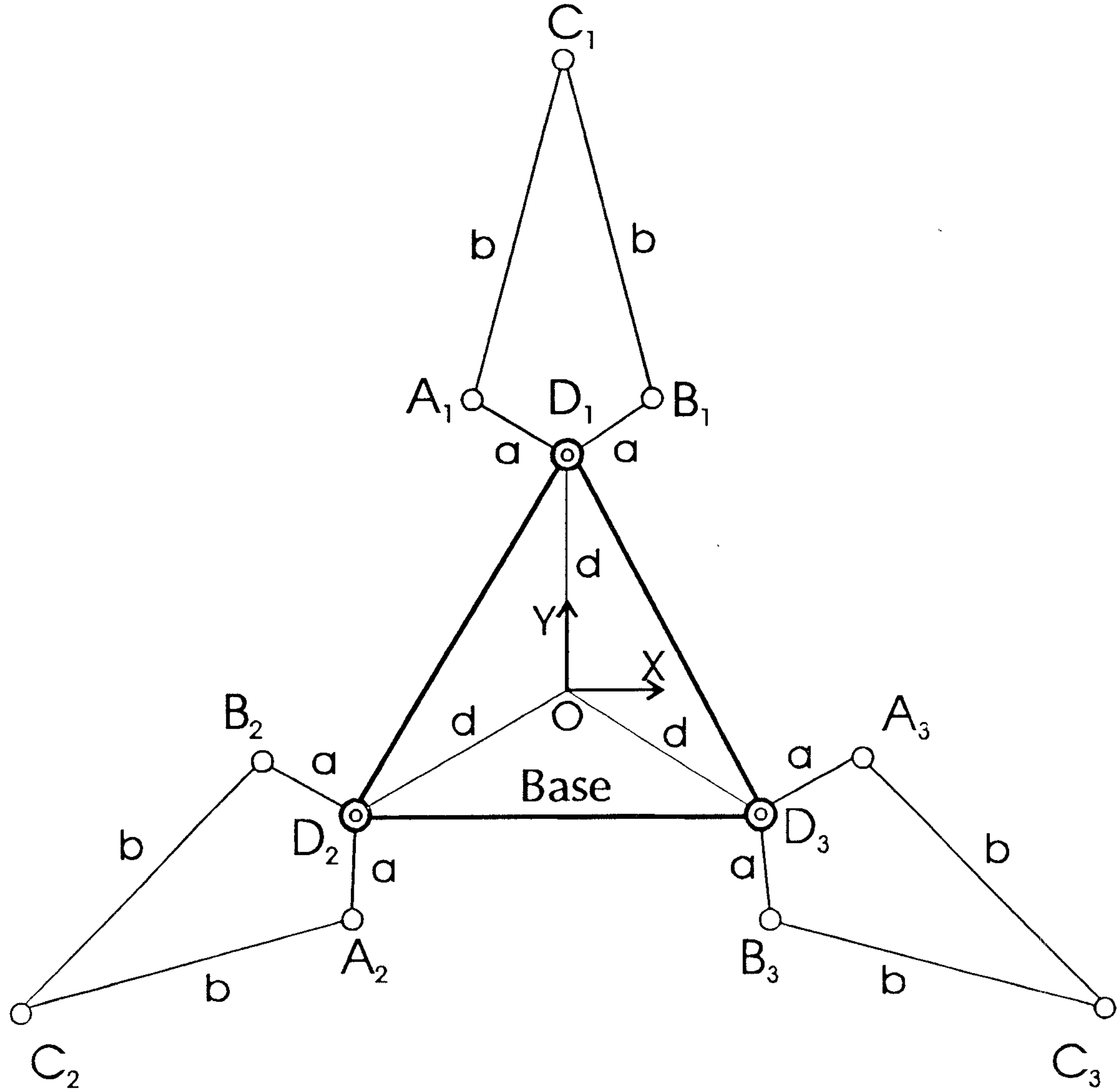


Figure 3 - Simplified Five-Bar Linkage Drivers

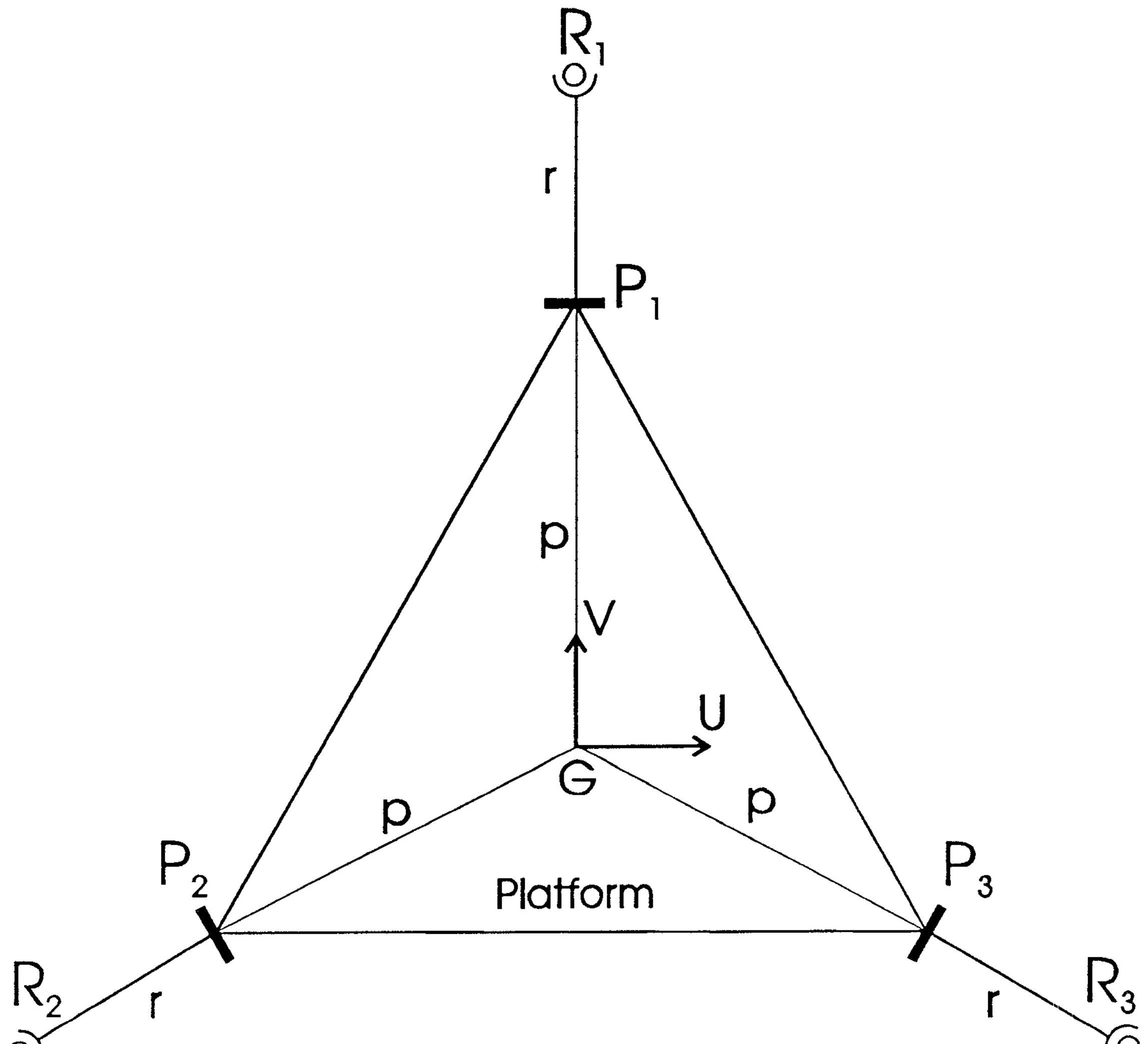


$R_1$, $R_2$, and $R_3$ are connected to drivers.

Figure 4 - Kinematic Equivalent of a Minimanipulator

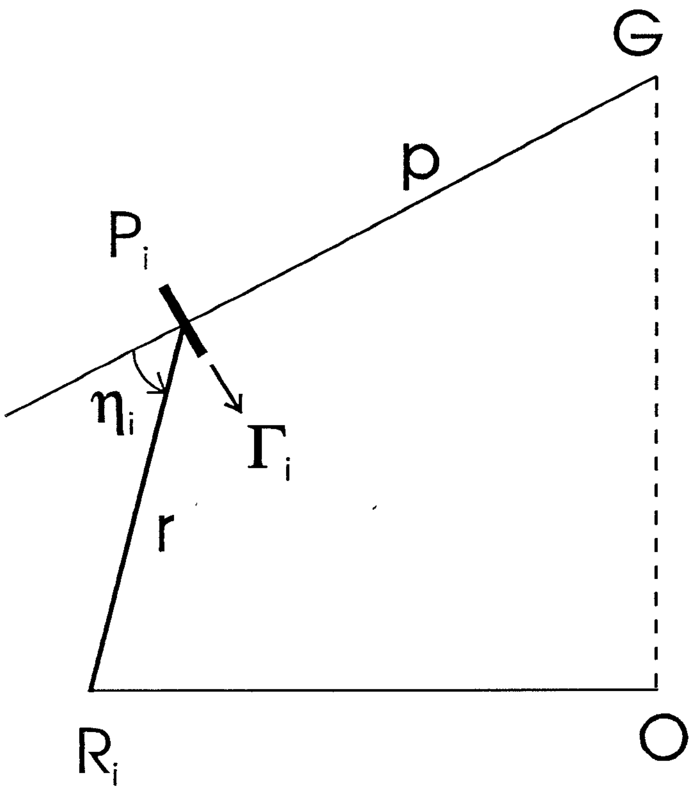


Figure 5 - Parameters Used in Jacobian Analysis

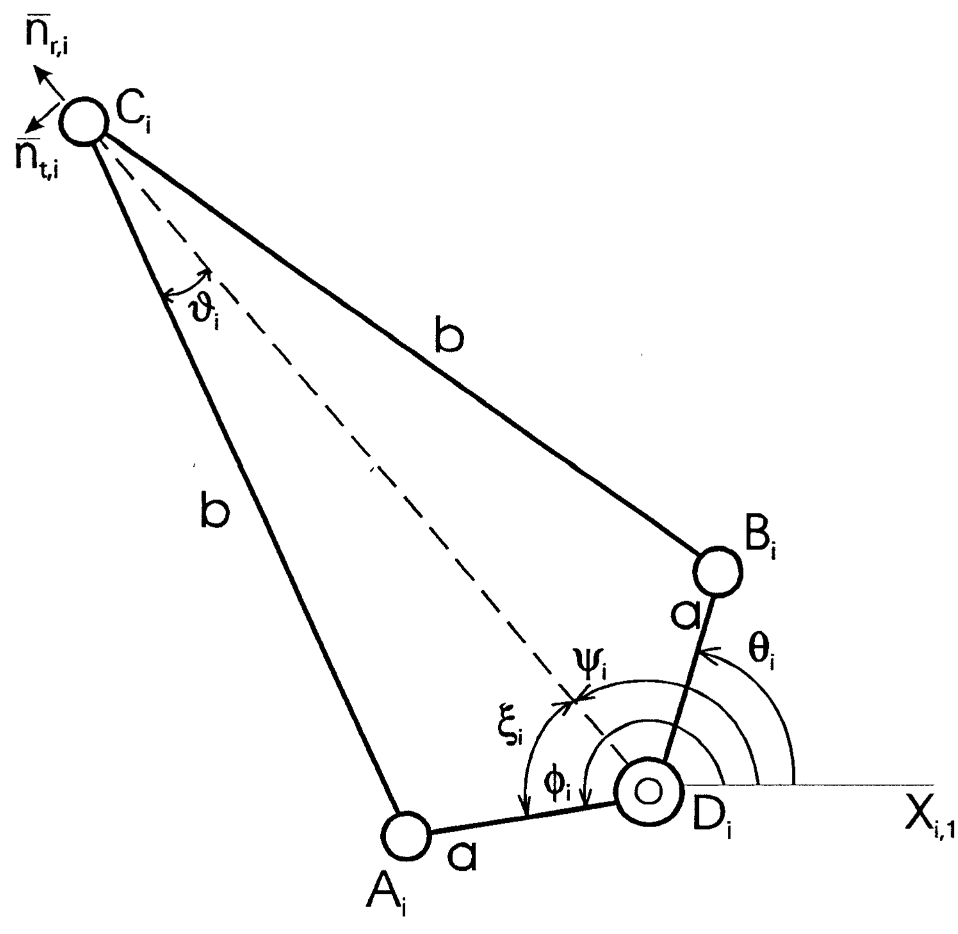


Figure 6 - Parameters Used in Velocity Analysis of Drivers